INTERNATIONAL TABLES FOR CRYSTALLOGRAPHY

ISSN 1574-8707
it.iucr.org

Volume I, X-ray Absorption Spectroscopy and Related Techniques
ISBN: 978-1-119-43394-1

XANES: theory and approaches

Takashi Fujikawa*

Graduate School of Advanced Integration Science, Chiba University, Yayoi-cho 1-33, Inage, Chiba, Japan. *Correspondence e-mail: tfujikawa@faculty.chiba-u.jp

A brief review of XANES theories is given which focuses on the basic theoretical framework rather than the technical details.

Keywords: XANES; theory.

1. Introduction

Several useful computer programs are now available for XAFS data analyses, which unfortunately means that we may have become unfamiliar with the basic theory behind them. Here, the theory of XAFS is briefly reviewed. A more comprehensive discussion is given by Rehr & Albers (2000). Here, we focus on the theoretical basic features of XANES analyses. There are several methods to calculate the X-ray absorption intensity $I(\omega)$ for excitation by monochromatic X-ray photons with energy ω. The basic method is given by the use of Fermi's golden rule,

$$I(\omega) = 2\pi \sum_{\rm f} |\langle {\rm f}|H_{\rm ep}|0\rangle|^2 \delta(E_0 + \omega - E_{\rm f}), \tag{1}$$

where $|0\rangle$ and $|{\rm f}\rangle$ are the initial and the final states of the target, with energies of E_0 and $E_{\rm f}$, respectively. The electron–photon interaction operator $H_{\rm ep}$ is written in the first and second quantizations,

$$H_{\rm ep} = \sum_i \Delta(\mathbf{r}_i) = \int {\rm d}x\, \psi^\dagger(x)\Delta(x)\psi(x),$$
$$x = (\mathbf{r}, \sigma), \tag{2}$$

where ψ and $\psi^\dagger$ are the electron annihilation and creation field operators. In the electric dipole (E1) approximation Δ is written for the linear polarization parallel to the z axis:

$$\Delta(\mathbf{r}) \propto rY_{10}(\hat{\mathbf{r}}). \tag{3}$$

For practical calculations of the ground state $|0\rangle$, some useful methods have been developed, for example Hartree–Fock (HF), density-functional theory (DFT) and configuration interaction (CI) methods; CI methods can also be applied to the final core-hole states $|{\rm f}\rangle$ (Kosugi *et al.*, 1984). The above direct approaches have been used to study XANES analyses excited from small systems such as molecules. For localized magnetic systems such as 3*d* transition-metal compounds or rare earths, multiplet and ligand field theory are quite useful to calculate both the $|0\rangle$ and $|{\rm f}\rangle$ states. These approaches provides us with simple physical pictures with low computational cost, but rely on semi-empirical calculations (van der Laan, 2006). The multichannel generalization of real-space multiple-scattering (MS) theory was developed to study XANES spectra by Natoli and coworkers (Natoli *et al.*, 1990). They combined MS theory and CI approaches, and discuss shake-up effects. It is however difficult to include bosonic excitations. Applications to $L_{2,3}$-edge XANES spectra show excellent

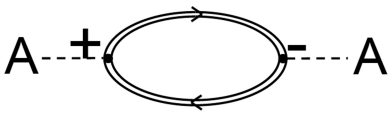

results for metallic and insulating Ca and Ti compounds (Krüger, 2018).

The formula (1) is not so convenient for handling large systems such as solids. We thus rewrite it

$$I(\omega) = -2\sum_{\rm f}|\langle 0|H_{\rm ep}|{\rm f}\rangle|^2 \times {\rm Im}\left(\frac{1}{E_0+\omega-E_{\rm f}+i\eta}\right) = -2{\rm Im}\langle 0|H_{\rm ep}G(E_0+\omega)H_{\rm ep}|0\rangle, \quad (4)$$

$$G(E) = \frac{1}{E-H+i\eta}, \quad (\eta \to +0). \quad (5)$$

This formula (4) is useful to derive multiple-scattering formula and is discussed in more detail in the next section. The formula (4) can also be written as an alternative expression,

$$I(\omega) = \int_{-\infty}^{\infty} {\rm d}t\, \langle 0|H_{\rm ep}(t)H_{\rm ep}|0\rangle \exp(i\omega t),$$
$$H_{\rm ep}(t) = \exp(iHt)H_{\rm ep}\exp(-iHt). \quad (6)$$

This correlation function formula is particularly useful to study many-body effects and phonon effects with aid of the Keldysh Green's function theory, which will be described later.

Two different approaches are discussed: many-body scattering theory and the Keldysh Green's function theory. Both have merits and also demerits.

2. X-ray absorption intensity

Here, we discuss the X-ray absorption intensity calculated by the use of formula (4). A basic theoretical framework, starting from many-body scattering theory, was developed by Hedin employing the quasi-boson approximation (Hedin, 1989). A more sophisticated approach beyond the quasi-boson approximation has been devised by Fujikawa (1999). These scattering theories based on projection-operator techniques have proven to be very powerful. Here, we provide an outline of these theories.

In order to study the deep core processes, we introduce a model Hamiltonian (Almbladh & Hedin, 1983),

$$H = H_{\rm v} + h + V + V_{\rm c}bb^\dagger + \varepsilon_{\rm c}b^\dagger b. \quad (7)$$

Here $H_{\rm v}$ is the full many-electron Hamiltonian for the valence electrons and $V_{\rm c}$ is the interaction between the core-hole and valence electrons, which is switched on only when the core hole is created. The effective one-electron Hamiltonian h describes the elastic scatterings, whereas V describes the inelastic scatterings inside solids. Within the present approximation the initial state of the target is written as the product $|0_{\rm v}\rangle|{\rm c}\rangle$, where $|0_{\rm v}\rangle$ is the ground state of a no-hole Hamiltonian, $H_{\rm v}|0_{\rm v}\rangle = E_0^{\rm v}|0_{\rm v}\rangle$, and b and $b^\dagger$ are the annihilation and creation operators, respectively, for the core level $|{\rm c}\rangle$. From equation (4) $H_{\rm ep}|0\rangle$ is written for the XANES analyses as

$$H_{\rm ep}|0\rangle = \sum_{\mathbf{k}}\langle\mathbf{k}|\Delta|{\rm c}\rangle c_{\mathbf{k}}^\dagger b|0_{\rm v}\rangle|{\rm c}\rangle = \sum_{\mathbf{k}}\langle\mathbf{k}|\Delta|{\rm c}\rangle c_{\mathbf{k}}^\dagger|0_v\rangle,$$

where $|\mathbf{k}\rangle$ is the photoelectron state which is the solution of $h|\mathbf{k}\rangle = \varepsilon_k|\mathbf{k}\rangle$ and $c_{\mathbf{k}}^\dagger$ is the creation operator for that state. Applying the approximate closure relation $\sum_{\mathbf{k}}|\mathbf{k}\rangle\langle\mathbf{k}| \simeq 1$, we have $H_{\rm ep}|0\rangle \simeq |0_{\rm v}\rangle\Delta|{\rm c}\rangle$, which yields

$$I(\omega) = -2{\rm Im}\langle{\rm c}|\Delta^* G(E)\Delta|{\rm c}\rangle,$$
$$G(E) = \langle 0_{\rm v}|(E-H_{\rm v}^*-h-V+i\eta)^{-1}|0_{\rm v}\rangle,$$
$$H_{\rm v}^* = H_{\rm v}+V_{\rm c},$$
$$E = E_0+\omega, \quad (\eta\to+0). \quad (8)$$

We should note that $G(E)$ is a one-electron operator in the photoelectron space because of h and V. By inserting the closure relation in core-hole space, $\sum_n |n_{\rm v}^*\rangle\langle n_{\rm v}^*| = 1$ ($H_{\rm v}^*|n_{\rm v}^*\rangle = E_n^{\rm v*}|n_{\rm v}^*\rangle$), and noticing that the intrinsic (shake-up) amplitude is given by $S_n = \langle n_{\rm v}^*|0_{\rm v}\rangle = \langle n_{\rm v}^*|b|0\rangle$, we can rewrite equation (8) as

$$I(\omega) = -2{\rm Im}\Big[\langle{\rm c}|\Delta^*\big(|S_0|^2\langle 0_{\rm v}^*|G_{\rm v}(E)|0_{\rm v}^*\rangle + \sum_{n\neq 0}[|S_n|^2\langle n^*|G_{\rm v}(E-\omega_n)|n_{\rm v}^*\rangle + S_n^*S_0\langle n_{\rm v}^*|G_{\rm v}(E)|0_{\rm v}^*\rangle + {\rm cc}] + \ldots\big)\Delta|{\rm c}\rangle\Big],$$
$$\omega_n = E_n^{\rm v*} - E_0^{\rm v*}, \quad (9)$$

where cc represents complex conjugation and $G_{\rm v}$ is defined as

$$G_{\rm v}(E) = (E-H_{\rm v}^*-h-V+i\eta)^{-1}. \quad (10)$$

We now apply the diagonal Green's function expansion developed by Hedin (Hedin, 1988; Fujikawa & Hedin, 1989) and then obtain a practical XAFS formula in terms of damping Green's function and extrinsic loss operators V_{nm} (Fujikawa, 1993; Campbell *et al.*, 2002),

$$I(\omega) = -2{\rm Im}\Big(|S_0|^2\langle{\rm c}|\Delta^* g_{\rm c}(\varepsilon)\Delta|{\rm c}\rangle + \sum_{n\neq 0}\big[|S_n|^2\langle{\rm c}|\Delta^* g_{\rm c}(\varepsilon-\omega_n)\Delta|{\rm c}\rangle + (S_n^*S_0\langle{\rm c}|\Delta^* g_{\rm c}(\varepsilon-\omega_n)V_{n0}g_{\rm c}(\varepsilon)\Delta|{\rm c}\rangle + {\rm cc})\big] + \ldots\Big),$$
$$V_{nm} = \langle n_{\rm v}^*|V_{\rm es}|m_{\rm v}^*\rangle, \quad (m\neq n),$$
$$\varepsilon = E_0^{\rm v} - E_0^{\rm v*} - \varepsilon_{\rm c} + \omega, \quad (11)$$

where $V_{\rm es}$ is the bare electron–target interaction. The first term in the large parentheses in equation (11) describes the main X-ray absorption band without intrinsic and extrinsic losses, the second term describes the intrinsic losses with probability $|S_n|^2$ and the third term describes the interference between them. Here, the purely extrinsic loss term is missing. To recover it careful analyses are necessary (Campbell *et al.*, 2002; Fujikawa & Niki, 2016). To study this problem, equation (11) is not so convenient because the optical potential $\Sigma_{\rm c}$ in equation (14) has some characteristic features around the loss thresholds. We thus rewrite the term in the large parentheses in equation (9) in terms of the core-hole excitation operator $X_{\rm c}$ defined by

$$X_{\rm c} = \sum_{n\neq 0}|n_{\rm v}^*\rangle(S_n/S_0)\langle 0_{\rm v}^*|. \quad (12)$$

The X-ray absorption intensity is now given by

$$I(\omega) = -2\mathrm{Im}[\langle \mathrm{c}|\Delta^* \langle 0_\mathrm{v}^*|G_0 + (G_0 V + X_\mathrm{c}^\dagger) \times G(VG_0 + X_\mathrm{c})|0_\mathrm{v}^*\rangle \Delta|\mathrm{c}\rangle],$$
$$G_0(E_0 + \omega) = (E_0 + \omega - H_\mathrm{v}^* - h_\mathrm{c} + i\eta)^{-1}. \quad (13)$$

The interference term $(VG_0 + X_\mathrm{c})|0_\mathrm{v}^*\rangle\Delta|\mathrm{c}\rangle$ suppresses the loss structure near the loss threshold (Hedin, 1989).

The damping propagator g_c for the core-hole potential is given by

$$g_\mathrm{c}(\varepsilon) = [\varepsilon - h_\mathrm{c} - \Sigma_\mathrm{c}(\varepsilon + E_0^*) + i\eta]^{-1},$$
$$h_\mathrm{c} = T_\mathrm{e} + \langle 0_\mathrm{v}^*|V_\mathrm{es}|0_\mathrm{v}^*\rangle, \quad (14)$$

where T_e is the kinetic energy operator for the photoelectron. An important factor to describe the photoelectron damping is the optical potential Σ_c, which is nonlocal, energy-dependent and non-Hermitian,

$$\Sigma_\mathrm{c}(E) = \langle 0^*|V_\mathrm{es} Q \frac{1}{E - H + i\eta} Q V_\mathrm{es}|0^*\rangle,$$
$$Q = 1 - |0^*\rangle\langle 0^*|. \quad (15)$$

Thus, the optical potential can explain the photoelectron mean free path, and can also have quite important effects on elastic photoelectron scatterings. A practical method to calculate the atomic optical potentials in solids has been developed within the GW approximation (Fujikawa *et al.*, 2000). This method has successfully been applied to depth distributions excited from solid surfaces (Shinotsuka *et al.*, 2008).

In the intrinsic approximation (the first and second terms in equation 11) we expect an abrupt jump in the X-ray absorption intensity at the loss threshold of the channel n above the absorption edge with energy ω_n. We have never observed such spike structures in the X-ray absorption near-edge structure (XANES or NEXAFS) region because of strong destructive interference (Hedin, 1989; Fujikawa, 1993). Detailed numerical calculations show that extrinsic and intrinsic losses tend to cancel near excitation thresholds, and correspondingly the strength of the main peak increases (Campbell *et al.*, 2002).

In addition to the many-body scattering theory, the Keldysh Green's function approach is quite useful in studying X-ray absorption processes (Fujikawa, 1999, 2001); this is discussed in Section 4.

3. Multiple-scattering theory

To derive the XAFS formula, we should notice that the core orbital φ_c is strongly localized on the X-ray-absorbing site A. In this case, we can pick up the following site T-matrix expansion of g_c.

$$g_\mathrm{c} = g_A + \sum_{\alpha\neq A} g_A t_\alpha g_A + \sum_{\alpha\neq\beta\neq A} g_A t_\beta g_0 t_\alpha g_A + \ldots, \quad (16)$$

where g_A is the scattering Green's function for the localized potential v_A on site A,

$$g_A(\varepsilon) = g_0(\varepsilon) + g_0(\varepsilon) t_A(\varepsilon) g_0(\varepsilon) = (\varepsilon - T_\mathrm{e} - v_A + i\eta)^{-1}.$$

The first term of equation (16) describes the isolated atomic absorption intensity, the second the single scattering ($A \rightarrow \alpha \rightarrow A$) and the third the double-scattering ($A \rightarrow \alpha \rightarrow \beta \rightarrow A$) terms. We assume that the incident X-rays are linearly polarized in the z direction: $\Delta \propto rY_{10}(\hat{\mathbf{r}})$. For the circular polarization propagating in the z direction, we have $\Delta_\pm \propto rY_{1,\pm1}(\hat{\mathbf{r}})$. The atomic absorption intensity σ_0 is now given in terms of the Gaunt integral $G(L_1L_2|L_3) = \int Y_{L_3}^*(\hat{\mathbf{r}}) Y_{L_1}(\hat{\mathbf{r}}) Y_{L_2}(\hat{\mathbf{r}})\,\mathrm{d}\hat{\mathbf{r}}$ and the radial integral ρ_c,

$$\sigma_0 \propto \frac{8k}{3} \sum_L \rho_\mathrm{c}(l)^2 G(L_\mathrm{c}10|L)^2,$$
$$\rho_\mathrm{c}(l) = \int \mathrm{d}r\, R_l(kr) R_{l_\mathrm{c}}(r) r^3, \quad L = (l, m), \quad (17)$$

where $\mathbf{k}$ is the wavevector of the photoelectron with energy $k^2/2$. The core function is not so influenced by the environment, and is written as $\varphi_\mathrm{c} = R_{l_\mathrm{c}}(r) Y_{L_\mathrm{c}}(\hat{\mathbf{r}})$. The radial part of the lth partial wave is $R_l(kr)$. From a selection rule for the Gaunt integral, the photoelectron angular momentum l is restricted to 1 when $l_\mathrm{c} = 0$ and to $l_\mathrm{c} \pm 1$ when $l_\mathrm{c} \geq 1$.

To calculate the single-scattering term $\langle \mathrm{c}|\Delta^* g_A t_\alpha g_A \Delta|\mathrm{c}\rangle$, we use the expansion in angular momentum applicable when $\mathbf{r} \in \alpha$ and $\mathbf{r}' \in A$ for a spherically symmetric potential v_A,

$$g_A(\mathbf{r}, \mathbf{r}'; k) = -2ik \sum_L h_l(kr) \exp(i\delta_l^A) R_l(kr') Y_L(\hat{\mathbf{r}}) Y_L^*(\hat{\mathbf{r}}'), \quad (18)$$

where $h_l(kr)$ is the lth spherical Hankel function and δ_l^A is the phase shift of the lth partial wave at site A. As $\mathbf{r} = \mathbf{r}_\alpha + \mathbf{R}_\alpha$ ($\mathbf{r}_\alpha = \mathbf{r} - \mathbf{R}_\alpha$), we can apply the origin-shift theorem (Rehr & Albers, 2000; Fujikawa, 2002),

$$-ikh_l(kr) Y_L(\hat{\mathbf{r}}) = \sum_{L'} G_{L'L}(k\mathbf{R}_\alpha) j_{l'}(kr_\alpha) Y_{L'}(\hat{\mathbf{r}}_\alpha) i^{l-l'}, \quad (19)$$

where $G_{LL'}$ is given by

$$G_{LL'}(k\mathbf{R}) = -4\pi ik \sum_{L_1} i^{l_1} h_{l_1}(kR) Y_{L_1}(\hat{\mathbf{R}}) G(L_1 L|L'). \quad (20)$$

We thus have a simple formula for the single-scattering term,

$$\sum_\alpha \langle \mathrm{c}|\Delta^* g_A t_\alpha g_A \Delta|\mathrm{c}\rangle \propto \frac{8\pi}{3} \sum_\alpha \sum_{LL'} i^{l-l'} \exp[i(\delta_l^A + \delta_{l'}^A)] \rho_\mathrm{c}(l) \rho_\mathrm{c}(l') \times G(L_\mathrm{c}10|L) G(L_\mathrm{c}10|L') \times \sum_{L_1} G_{LL_1}(-k\mathbf{R}_\alpha) t_{l_1}^\alpha(k) G_{L_1L'}(k\mathbf{R}_\alpha), \quad (21)$$

where t_l^α is the angular momentum representation of the site T-matrix at α, which can be written in terms of the phase shift δ_l^α of the lth partial wave

$$t_l^\alpha(k) = -[\exp(2i\delta_l^\alpha) - 1]/(2ik). \quad (22)$$

In the same way, the nth-order multiple-scattering term can be given in terms of the same ingredients,

$$\sum_{\alpha_n \alpha_{n-1} \ldots \alpha_1} \langle \mathrm{c}|\Delta^* g_A t_{\alpha_n} g_0 t_{\alpha_{n-1}} \ldots g_0 t_{\alpha_1} g_A \Delta|\mathrm{c}\rangle \propto \frac{8\pi}{3} \sum_{m_\mathrm{c} LL'} i^{l-l'} \exp[i(\delta_l^A + \delta_{l'}^A)] \rho_\mathrm{c}(l) \rho_\mathrm{c}(l') \times G(L_\mathrm{c}10|L) G(L_\mathrm{c}10|L') (GX^n)_{LL'}^{AA}. \quad (23)$$

We have introduced a matrix labelled by site indices and orbital angular momentum,

$$X^{\alpha\beta}_{LL'} = t^{\alpha}_{l}(k)G_{LL'}(k\mathbf{R}_{\alpha} - k\mathbf{R}_{\beta})(1-\delta^{\alpha\beta}). \quad (24)$$

Using these matrices, we can renormalize the full multiple-scattering series to infinite order, atomic + single + double + $\ldots$ + ∞, by noting that $t^{\alpha\beta}_{LL'} = \delta^{\alpha\beta}\delta_{LL'}t^{\alpha}_{l}$,

$$\sigma^{\infty} \propto -\frac{8}{3}\mathrm{Im}\Big\{ \sum_{m_c LL'} i^{l-l'} \exp[i(\delta^{A}_{l} + \delta^{A}_{l'})]\rho_c(l)\rho_c(l') \times G(L_c 10|L)G(L_c 10|L')[(t - Xt)^{-1}]^{AA}_{LL'} \Big\}. \quad (25)$$

This formula can be applied to XANES analyses. In equation (24) the T-matrix t^{α}_{l} reflects the electronic structure at site α, whereas the propagator $G_{LL'}(k\mathbf{R}_{\alpha} - k\mathbf{R}_{\beta})$ reflects the details of the atomic arrangements inside the cluster that we are considering. In equation (25) we take the sum over L and L'; however, the maximum l and l' become larger for larger k ($l_{\max} \propto k$). In the XANES region $l_{\max}$ is quite small: typically less than 5. When we take up to g waves and 40 atoms into account, the dimension of the matrix X defined by equation (24) amounts to 1000. This multiple renormalization technique is only applicable in the low-energy region: the XANES region. In contrast, $l_{\max}$ amounts to $\sim$20 in the extended X-ray absorption fine-structure (EXAFS) region.

In the high-energy limit, the propagator $G_{LL'}$ given by equation (20) has a simple asymptotic form

$$G_{LL'}(k\mathbf{R}) \simeq -4\pi\frac{\exp(ikR)}{R}Y^{*}_{L}(\hat{\mathbf{R}})Y_{L'}(\hat{\mathbf{R}}), \quad (26)$$

which yields the well known plane-wave EXAFS formula from equation (21). More sophisticated approaches to finite multiple scatterings have been developed on the basis of the z-axis propagator developed by Fritzsche (1990) and Rehr & Albers (1990). The real-space multiple-scattering approaches shown above can be applied to all types of molecules, liquids and solids as long as we have adequately good models.

The explicit XANES formula (25) is based on spherical atomic potentials (muffin-tin potentials). Extensions to general shape atomic potentials have been devised by several authors, and some codes are now available (Hatada & Natoli, 2018). For XANES analyses excited from strongly anisotropic systems, the full-potential effects play an important role.

Instead of real-space approaches, we can use Bloch wave approaches for crystalline solids. Neglecting the many-body effects in equation (11), we have

$$I(\omega) \simeq -2\mathrm{Im}|S_0|^2\langle \mathrm{c}|\Delta^{*}g_{\mathrm{c}}(\varepsilon)\Delta|\mathrm{c}\rangle, \quad (27)$$

$$g_{\mathrm{c}}(\varepsilon) \simeq (\varepsilon - h_{\mathrm{c}} + i\eta)^{-1} = \sum_{i}\frac{|\varphi_i\rangle\langle\varphi_i|}{\varepsilon - \varepsilon_i + i\eta}, \quad (28)$$

where $|\varphi_i\rangle$ is the solution of the one-electron equation $h_{\mathrm{c}}|\varphi_i\rangle = \varepsilon_i|\varphi_i\rangle$. We should note that h_{c} includes the core-hole effects. For ordered solids, Bloch functions are used in the HF and DFT methods. Some codes are widely used for practical band calculations, which are implemented to calculate XANES spectra (see, for example, Minar *et al.*, 2018). In order to consider the core-hole effects, they usually use supercells to isolate the X-ray-absorbing atom. The supercell has to be large enough to minimize the interaction between the absorbing atom and its periodically repeated atoms.

The renormalized multiple-scattering XANES formula (equation 11) has the damping one-electron Green's function g_{c} given by equation (14). The one-electron Hamiltonian h_{c} has static hole potential $\langle 0^{*}_{\mathrm{v}}|V_{\mathrm{es}}|0^{*}_{\mathrm{v}}\rangle$, which is given by the sum of the Hartree potential and the exchange potential. The former is directly calculated within muffin-tin (MT) or non-MT approaches, whereas the latter is usually calculated by the use of some local density approximations. Slater averaged this exchange contribution for electrons below the Fermi level, and assumed that the exchange potential in a solid could be approximated by a local potential where the constant electron density n is replaced by the electron density $n(\mathbf{r})$, which yields the local exchange potential (Slater, 1951),

$$v_{\mathrm{ex}}(\mathbf{r}) \simeq -\frac{3}{2}\left[\frac{3n(\mathbf{r})}{\pi}\right]^{1/3}. \quad (29)$$

This potential is widely used, not only for electrons below the Fermi level, but also in scattering problems, where it is basically incorrect. Thus for high energies exchange scattering can be neglected, whereas the Slater exchange potential still has an influence. A more widely used variant of v_{ex} is the X_{α} potential, $v_{X\alpha} = \alpha v_{\mathrm{ex}}$.

For scattering problems, the exchange potential before averaging is more motivated. This potential is local and energy-dependent and decays at high energy; it was shown by Hara to be successful for electron scattering from atoms and molecules (Hara, 1967). It is often called the Dirac–Hara potential.

These methods employ the HF approximation for a uniform electron gas. Hedin and Lundqvist suggested a scheme in which the electron-gas self-energy in the GW approximation $\Sigma_{\mathrm{GW}}(q, \varepsilon)$ is used with an $\mathbf{r}$-dependent momentum $q(\mathbf{r})$ (Hedin & Lundqvist, 1971). Lee and Beni applied such a potential to EXAFS, using the plasmon pole approximation, and showed that this potential gives excellent results (Lee & Beni, 1977).

We can show that the optical potential Σ_{c} defined by equation (15) is approximately equivalent to the self-energy in the GW approximation (Fujikawa & Hedin, 1989). A practical method to calculate the atomic optical potential is thus developed based on the GW approximation. Both the polarization P and the one-electron Green's function G can be split into core and valence parts. The core polarization is assumed to be much smaller than the valence polarization P^{v}. We then have an expansion in powers of P^{c} for the self-energy (Hedin & Lundqvist, 1970),

$$\Sigma_{\mathrm{c}} = G^{\mathrm{v}}W^{\mathrm{v}} + V^{\mathrm{c}}_{\mathrm{ex}} + G^{\mathrm{v}}W^{\mathrm{v}}P^{\mathrm{c}}W^{\mathrm{v}} + \ldots. \quad (30)$$

Here $G^{\mathrm{v}}W^{\mathrm{v}}$ is the self-energy from the valence (itinerant) electrons, while $V^{\mathrm{c}}_{\mathrm{ex}}$ is the bare exchange and $G^{\mathrm{v}}W^{\mathrm{v}}P^{\mathrm{c}}W^{\mathrm{v}}$ is the screened polarization potential from the ion cores. We can calculate $G^{\mathrm{v}}W^{\mathrm{v}}$ by use of the Hedin–Lundqvist potential and $V^{\mathrm{c}}_{\mathrm{ex}}$ by use of the local density approximation discussed previously. The polarization potential $V_{\mathrm{pol}} = G^{\mathrm{v}}W^{\mathrm{v}}P^{\mathrm{c}}W^{\mathrm{v}}$ can be approximated by use of the average excitation energy Δ,

$$V_{\mathrm{pol}}(x, x'; \omega) = A(\mathbf{r}, \mathbf{r}')G^{\mathrm{v}}(x, x'; \omega - \Delta). \quad (31)$$

The valence Green's function G^{v} is energy-dependent; we should note that the energy $\omega - \Delta$ is used here. The static polarization potential A is not energy-dependent. These nonlocal self-consistent optical potentials are applied to electron–atom elastic scatterings, which demonstrate satisfactory agreement with the observed results (Fujikawa *et al.*, 2000).

4. Phonon effects

Among phonon effects on XAFS, the EXAFS Debye–Waller factors have extensively been studied (Fornasini, 2012), whereas other factors such as Franck–Condon factors and electron–phonon interactions are rarely discussed. Ankudinov and Rehr have shown that local atomic displacements are responsible for additional XANES peaks (Ankudinov & Rehr, 2005). They used a simple formula for the X-ray absorption intensity $I(\omega, Q)$ considering the thermal average shown by $\langle \ldots \rangle$,

$$\langle I(\omega, Q)\rangle = I(\omega, Q_0) + \frac{1}{2}\sum_{\alpha i}\sum_{\beta j}\langle u_{i\alpha}u_{j\beta}\rangle\left[\frac{\partial^2 I(\omega, Q)}{\partial u_{i\alpha}\partial u_{j\beta}}\right]_0, \quad (32)$$

where Q designates the assembly of nuclei $Q = (\mathbf{R}_\alpha, \mathbf{R}_\beta, \ldots)$. The above equation takes a small deviation from the equilibrium atomic configuration $Q_0 (u = Q - Q_0)$. The first-order terms cancel since $\langle u_{i\alpha}\rangle = 0$, $(i = x, y, z)$. For solids the summation over atomic sites α, β, ... runs over all nearby composite atoms.

A prominent temperature-dependence of the pre-edge structures is observed in Ti K-edge XANES of $SrTiO_3$ from 15 to 300 K. One of the pre-edge peaks shows an increase in intensity with temperature (Nozawa *et al.*, 2005). Manuel and coworkers presented the Al K-edge XANES spectra of corundum and beryl in the temperature range 300–930 K (Manuel *et al.*, 2012). These experimental results provide evidence of the role of thermal fluctuation in XANES at the Al K edge: the pre-edge grows and shifts to lower energy with temperature. They used DFT calculations for both compounds and demonstrated that the pre-edge peak originates from the dipole-forbidden $1s \rightarrow 3s$ transition. The theoretical analyses used are based on previous papers (Cabaret & Brouder, 2009; Brouder *et al.*, 2010). Nemausat and coworkers incorporated the nuclear motion by generating several non-equilibrium configurations from the dynamical matrix within the Born–Oppenheimer and quasi-harmonic approximations (Nemausat *et al.*, 2015). The averaged calculated Mg K XANES spectra in MgO have been compared with experimental data, and show satisfactory agreement.

Here, a theory developed by Fujikawa and coworkers is outlined to illustrate how to apply the Keldysh Green's function technique to XANES analyses (Fujikawa *et al.*, 2015). The X-ray absorption intensity $I(\omega)$ at $T = 0$ K is given by the correlation function (see equation 6),

$$I(\omega) = \int \mathrm{d}x\,\mathrm{d}x'\,\Delta^*(x)\Delta(x') \times \int_{-\infty}^{\infty} \mathrm{d}t\,\langle 0|n(xt)n(x')|0\rangle \exp(i\omega t), \quad (33)$$

where $n(x) = \psi^\dagger(x)\psi(x)$, $[x = (\mathbf{r}, \sigma)]$. The last expression is obtained in dipole length and acceleration forms.

The above formula is extended to finite temperature by use of the thermal average instead of the average over the ground state $|0\rangle$. The reducible polarization propagator $\pi^>$ is given by

$$i\pi^>(1, 2) = \langle \delta n(1)\delta n(2)\rangle = \langle n(1)n(2)\rangle - \langle n(1)\rangle\langle n(2)\rangle, \quad (34)$$

where $\delta n(1) = n(1) - \langle n(1)\rangle$ is the electron-density fluctuation. The second term in the last expression makes no contribution to photo-excitation because the time integration in equation (33) gives rise to the factor $\delta(\omega)$. We thus obtain an expression for the X-ray absorption intensity,

$$I(\omega) = i\int \mathrm{d}x\,\mathrm{d}x'\,\Delta^*(x)\Delta(x') \times \int_{-\infty}^{\infty} \mathrm{d}t\,\pi^>(xt, x')\exp(i\omega t). \quad (35)$$

The reducible polarization π is given in terms of irreducible polarization P and the screened Coulomb interaction W (Hedin & Lundqvist, 1970),

$$\pi(1, 2) = P(1, 2) + \int_c \mathrm{d}3\,\mathrm{d}4\,P(1, 3)W(3, 4)P(4, 2). \quad (36)$$

The time integrals along the Keldysh contour are denoted as $\int_c \ldots$. The lowest order approximation in the skeleton expansion gives

$$i\pi^>(xt, x') \simeq iP^>(xt, x') \simeq g^>(xt, x')g^<(x', xt). \quad (37)$$

The greater one-electron Green's function $g^>$ describes the propagation of excited photoelectrons and the lesser one-electron Green's function $g^<$ describes hole propagation. We should notice that both already include some correlation effects and phonon effects.

In the core-excitation processes the latter is well approximated by use of the model Hamiltonian (equation 7) and we have

$$ig^<(x', xt) = -\langle \psi^\dagger(xt)\psi(x')\rangle \simeq -\langle \varphi_c^*(x)\varphi_c(x')b^\dagger(t)b\rangle. \quad (38)$$

The thermal average in equation (38) is taken over electronic and phonon states. As shown below, $\varphi_c(\mathbf{r})$ (spin effects will be neglected in this section) still depends on phonon states. From now on we will use the Born–Oppenheimer approximation for simplicity. The core function φ_c is well approximated by

$$\begin{aligned}\varphi_c(\mathbf{r}) &= \varphi_c(\mathbf{r} - \mathbf{R}_A^0 - \mathbf{u}_A),\\ \varphi_c(\mathbf{r}) &= R_{l_c}(r)Y_{L_c}(\hat{\mathbf{r}}),\end{aligned} \quad (39)$$

where $\mathbf{R}_A^0$ is the equilibrium position of the X-ray-absorbing atom A and $\mathbf{u}_A$ is the deviation from it. For the small deviation, we have

$$\varphi_c(\mathbf{r} - \mathbf{R}_A^0 - \mathbf{u}_A) = \sum_L \varphi_L^c(\mathbf{r} - \mathbf{R}_A^0)J_{LL_c}(\mathbf{u}_A). \quad (40)$$

Even if the core function is a $1s$ function, phonon vibrations yield nonspherical contributions as shown above.

Here, the full Hamiltonian H includes the phonon Hamiltonian $H_{\rm vib}$ in addition to the electronic Hamiltonian $H_{\rm e}$ given by equation (7),

$$H = H_{\rm e} + H_{\rm vib} = H_{\rm e}^{*} + H_{\rm vib}^{*},$$
$$H_{\rm e}^{*} = H_{\rm v}^{*} + V_{\rm c}, \tag{41}$$

where $H_{\rm vib}$ is the phonon Hamiltonian with no core hole and $H_{\rm vib}^{*}$ is the phonon Hamiltonian with a core hole on $\varphi_{\rm c}$, which is given in the linear displacement approximation,

$$H_{\rm vib}^{*} = H_{\rm vib} + \sum_{\nu}(B_{\nu}a_{\nu} + B_{\nu}^{*}a_{\nu}^{\dagger}), \quad \nu = (\mathbf{q}, j),$$

where $\mathbf{q}$ is the crystal momentum and j is the phonon branch. We thus have a useful expression for the hole propagator $g^{<}$ with the aid of equation (40),

$$ig^{<}(\mathbf{r}', \mathbf{r}t) = -\sum_{LL'}\varphi_{L}^{\rm c}(\mathbf{r} - \mathbf{R}_{A}^{0})\varphi_{L'}^{\rm c}(\mathbf{r}' - \mathbf{R}_{A}^{0}) \times \langle J_{LL_{\rm c}}^{*}(\mathbf{u}_{A})J_{L'L_{\rm c}}(\mathbf{u}_{A})\exp(iH_{\rm vib}t) \times \exp(-iH_{\rm vib}^{*}t)\rangle_{\rm vib}\langle\exp(iH_{\rm e}t)\exp(-iH_{\rm e}^{*}t)\rangle_{\rm e}, \tag{42}$$

where $\langle\ldots\rangle_{\rm vib}$ and $\langle\ldots\rangle_{\rm e}$ are the averages over phonon states and electron states, respectively.

We now use some simple approximations: $H_{\rm vib} = H_{\rm vib}^{*}$ (the difference of $H_{\rm vib}$ and $H_{\rm vib}^{*}$ can contribute to Franck–Condon effects) and the harmonic approximation for the phonon Hamiltonian $H_{\rm vib}$, which yields

$$\langle J_{LL_{\rm c}}^{*}(\mathbf{u}_{A})J_{L'L_{\rm c}}(\mathbf{u}_{A})\rangle_{\rm vib} \simeq 4\pi(-1)^{l'+l_{\rm c}}\exp(a^{2}\sigma_{A}^{2}) \times \sum_{L_{1}} i^{l_{1}}j_{l_{1}}(ia^{2}\sigma_{A}^{2})G(L_{\rm c}L_{1}|L) \times G(L_{\rm c}L_{1}|L'), \tag{43}$$

where a is the exponent of the core function $R_{l_{\rm c}}(r)$ and σ_{A}^{2} is the averaged thermal fluctuation of the X-ray-absorbing atom A given by

$$\sigma_{A}^{2} = \langle\mathbf{u}_{A}^{2}\rangle_{\rm vib}/3.$$

The most important term in the above sum in equation (43) arises from the term with $l_1 = 0$ and the next is from the term with $l_1 = 1$, because $a^{2}\sigma_{A}^{2} \ll 1$. We thus have an interesting formula for the hole Green's function for deep core excitation from $\varphi_{\rm c}$ where atomic thermal motions are taken into account,

$$ig^{<}(\mathbf{r}', \mathbf{r}t) = \Big[-\varphi_{L_{\rm c}}^{\rm c*}(\mathbf{r} - \mathbf{R}_{A}^{0})\varphi_{L_{\rm c}}^{\rm c}(\mathbf{r}' - \mathbf{R}_{A}^{0})j_{0}(ix) + 4\pi i\sum_{LL'}\varphi_{L}^{\rm c*}(\mathbf{r} - \mathbf{R}_{A}^{0})\varphi_{L'}^{\rm c}(\mathbf{r}' - \mathbf{R}_{A}^{0})j_{1}(ix) \times \sum_{m_1} G(L_{\rm c}1m_{1}|L)G(L_{\rm c}1m_{1}|L') + \ldots\Big]\exp(x) \times \langle\exp(iH_{\rm e}t)\exp(-iH_{\rm e}^{*}t)\rangle_{\rm e}, \tag{44}$$

where $x = a^{2}\sigma_{A}^{2}$ and $j_l(x)$ is the spherical Bessel function. The first term describes the excitation from the core function with the same orbital angular momentum $l_{\rm c}$; the thermal vibrations have influenced the weight from 1 to $\exp(x)j_0(ix)$. The second term in the large square brackets is simplified for the K-edge excitation ($l_{\rm c} = 0$),

$$\sum_{m_1}\varphi_{1m_1}^{\rm c*}(\mathbf{r} - \mathbf{R}_{A}^{0})\varphi_{1m_1}^{\rm c}(\mathbf{r}' - \mathbf{R}_{A}^{0})j_{1}(ix). \tag{45}$$

The thermal motion thus gives rise to the excitation from a p-type core orbital.

So far, we have focused on the hole propagator $g^{<}$. Next, we investigate the particle propagator $g^{>}$. A useful expression is given in terms of the particle Dyson orbital f_q,

$$ig^{<}(\mathbf{r}t, \mathbf{r}') = \sum_{q} f_{q}(\mathbf{r})f_{q}^{*}(\mathbf{r}')\exp(-i\varepsilon_{q}t),$$
$$f_{q}(\mathbf{r}) = \langle N, 0|\psi(\mathbf{r})|N+1, q\rangle,$$
$$\varepsilon_{q} = E_{q}(N+1) - E_{0}(N). \tag{46}$$

In a one-electron approximation the particle Dyson orbital f_q is reduced to the corresponding excited orbital or continuum photoelectron wavefunction with damping. Substituting equations (37), (42) and (44) into equation (35), we obtain a useful formula to describe the pre-edge structures in K-edge X-ray absorption spectra where Franck–Condon effects are neglected,

$$I(\omega) = 2\pi\exp(x)\sum_{q}\Big[|\langle f_{q}|\Delta|\varphi_{1s}\rangle|^{2}j_{0}(ix) + \sum_{m}|\langle f_{q}|\Delta|\varphi_{1m}^{1s}\rangle|^{2}j_{1}(ix) + \ldots\Big]A_{c}(\varepsilon_{q} - \omega),$$
$$A_{c}(\varepsilon) = \sum_{n}|S_{n}|^{2}\delta(\varepsilon - \varepsilon_{n}), \quad (x = a^{2}\sigma_{A}^{2}). \tag{47}$$

The first term is the conventional X-ray absorption intensity for the $1s \rightarrow f_q$ transition, which has phonon effects in the factor $\exp(x)j_0(ix)$. The second describes the absorption intensity induced by atomic displacement due to thermal motion. We have an explicit expression for the electron–photon interaction operator Δ neglecting the unimportant numerical factor,

$$\Delta = \Delta_{\rm E1} + \Delta_{\rm E2} + \ldots,$$
$$\Delta_{\rm E1} = \mathbf{e}\cdot\mathbf{r}, \quad \Delta_{\rm E2} = \frac{i}{2}(\mathbf{e}\cdot\mathbf{r})(\mathbf{k}\cdot\mathbf{r}), \tag{48}$$

where $\Delta_{\rm E1}$ is the electric dipole (E1) and $\Delta_{\rm E2}$ is the electric quadrupole (E2); $\mathbf{e}$ and $\mathbf{k}$ are the photon polarization and propagation vectors. We notice that $|\mathbf{e}| = 1$, $\omega = ck$ and $\mathbf{e}\cdot\mathbf{k} = 0$. The multipole transition operators in the relativistic theory are discussed in Section 5.

Now we consider $1s \rightarrow 3d$ transitions in transition-metal atoms that have vacant $3d$ levels. When we consider the $1s \rightarrow 3d$ excitation, only the E2 transition is allowed in the static approximation, which should be quite small. When we take the atomic thermal motion into account, the E1 transition $\varphi_{1m}^{1s} \rightarrow 3d$ (the second term in equation 47) is also allowed. Some numerical calculations show that the pre-edge intensity increases with temperature, which is in accordance with the observed results. For small σ_A the temperature-dependence is a linear function of the temperature T and the E1 and E2 transitions are of the same order; however, a nonlinear temperature-dependence is observed and the E1 transition is dominant for large σ_A (Fujikawa *et al.*, 2015).

Above the K edge, we directly use $g^{>}$ instead of the particle Dyson orbitals f_q to describe the photoelectron propagation. In the formula $\mathrm{Im}\langle\varphi_c|\Delta^* g^{>}\Delta|\varphi_c\rangle$, we can replace $g^{>}$ by $2g^{r}$ (the retarded Green's function). The XANES formula is now reduced to

$$I(\omega) = -\frac{1}{\pi}\mathrm{Im}\Big[\langle\varphi_{1s}|\Delta^* g^{r}(\varepsilon)\Delta|\varphi_{1s}\rangle j_0(ix) + \sum_m \langle\varphi_{1m}^{1s}|\Delta^* g^{r}(\varepsilon)\Delta|\varphi_{1m}^{1s}\rangle j_1(ix)\Big]\exp(x). \quad (49)$$

The retarded Green's function g^{r} plays the same role as the scattering Green's function g_c because of the identical boundary condition. We can apply the multiple-scattering theory as discussed previously to both the first and second terms in equation (49).

Even in the XANES region, the Debye–Waller factors are important to study the temperature-dependence, although they are not as prominent compared with EXAFS Debye–Waller factors because of the small k in the XANES region. For XANES analyses excited from systems with large disorder, the XANES Debye–Waller factors should play an important role. In the low-energy region spherical wave effects are crucial. With the aid of formula (40), the temperature-dependent path matrix from the α site to the β site is now given by

$$X_{LL'}^{\beta\alpha}(T) = \sum_{L_1} X_{LL_1}^{\beta\alpha} K_{L_1L'}^{\beta\alpha}(T),$$
$$K_{L_1L'}^{\beta\alpha}(T) = \int \mathrm{d}\hat{\mathbf{r}}\, Y_{L_1}^*(\hat{\mathbf{r}}) \times \exp\left\{-\frac{k^2}{2}\langle[(\mathbf{u}_\beta - \mathbf{u}_\alpha)\cdot\hat{\mathbf{r}}]^2\rangle\right\} Y_{L'}(\hat{\mathbf{r}}), \quad (50)$$

where X is given by equation (24).

5. Relativistic XANES theory

As is well known, the influence of relativistic effects increases with the atomic number Z. To date, several relativistic XAFS theories have been investigated using perturbation approaches, which have successfully been applied to XAFS from light elements (Brouder & Hikam, 1991). Gesztesy and coworkers have developed a useful approach to represent the Dirac Green's function in terms of a full nonrelativistic Green's function (Gesztesy *et al.*, 1984). An alternative theoretical approach has been developed to study relativistic effects on XANES spectra (Ankudinov & Rehr, 1997). They solved the Dirac equation for limiting cases and arrived at an interpolation scheme that allows one to circumvent the solution of the coupled radial Dirac equation, which occurs within a fully relativistic scheme. A fully relativistic theory for magnetic EXAFS has been presented based on the Dirac equation for spin-polarized systems (Ebert *et al.*, 1999). For X-ray magnetic circular dichroism (XMCD) relativistic effects are essential, in particular due to spin–orbit interaction. Some useful review articles have been published (Ebert, 1996; Wende, 2004).

The X-ray absorption intensity is given for excitation from the core-level 4-spinor $|\mathrm{c}\rangle$ similar to equation (8), where $|\mathrm{c}\rangle$ is the 2-spinor,

$$I(\omega) = -2\mathrm{Im}\langle\mathrm{c}|(\alpha\cdot\mathbf{A})^{\dagger} G_{\mathrm{D}}(\varepsilon)(\alpha\cdot\mathbf{A})|\mathrm{c}\rangle. \quad (51)$$

Here, α_k ($k = x, y, z$) are the Dirac matrices, $\mathbf{A}$ is the vector potential of the incident X-ray, ε is the kinetic energy of photoelectrons and ω is the X-ray photon energy.

The core state $|\mathrm{c}\rangle$ can be written in terms of the 2-spinor φ_c (large component) and χ_c (small component),

$$|\mathrm{c}\rangle = \begin{pmatrix} |\varphi_c\rangle \\ |\chi_c\rangle \end{pmatrix},$$
$$\varphi_c(\mathbf{r}) = g_{l_c}(r) y_{j_c\mu_c}^{l_c}(\hat{\mathbf{r}}),$$
$$\chi_c(\mathbf{r}) = i f_{l_c}(r)\sigma\cdot\hat{\mathbf{r}} y_{j_c\mu_c}^{l_c}(\hat{\mathbf{r}}). \quad (52)$$

The Pauli spinors $y_{j_c\mu_c}^{l_c}(\hat{\mathbf{r}})$ are simultaneous eigenstates of J^2, L^2, S^2 and J_z ($\mathbf{J} = \mathbf{L} + \mathbf{S}$). We can obtain the radial functions g_{l_c} and f_{l_c} by solving the one-electron Dirac equation.

The Foldy–Wouthuysen (FW) transformation provides us with a useful connection between nonrelativistic and relativistic quantum theory (Schwable, 2008). Bouldi & Brouder (2017) derived a relativistic XAFS formula and have shown that the interaction operator $\alpha\cdot\mathbf{A}$ is rewritten for absorption,

$$\alpha\cdot\mathbf{A} = \begin{pmatrix} \Delta_1 & 0 \\ 0 & \Delta_1 \end{pmatrix} + \begin{pmatrix} 0 & \Delta_2 \\ \Delta_2 & 0 \end{pmatrix}, \quad (53)$$

where $\Delta_1 = \Delta_{E1} + \Delta_{E2}$, as given by equation (48), and Δ_2 is

$$\Delta_2 = \frac{1}{2\omega}(\mathbf{e}\times\mathbf{k})\cdot(\mathbf{r}\times\sigma).$$

Bouldi and Brouder have also shown that the relativistic formula for the X-ray absorption intensity (equation 51) can be rewritten on the basis of the FW transformation, which is given only in terms of the large component $|\varphi_c\rangle$,

$$I(\omega) = -2\mathrm{Im}\langle\varphi_c|\Delta^{\dagger} g(\varepsilon)\Delta|\varphi_c\rangle, \quad (54)$$

$$\Delta = \Delta_1 + \Delta_{M1} + \Delta_{SP}. \quad (55)$$

Here, Δ_{M1} is the magnetic dipole transition operator and Δ_{SP} is the spin–position operator introduced by Bouldi and Brouder,

$$\Delta_{M1} = \frac{1}{2c\omega}(\mathbf{e}\times\mathbf{k})\cdot(\mathbf{L}+\sigma),$$
$$\Delta_{SP} = \frac{i\omega}{4c^2}(\mathbf{e}\times\mathbf{r})\cdot\sigma. \quad (56)$$

We should note that the nonrelativistic Green's function $g(\varepsilon)$ additionally has spin–orbit interaction because of the FW transformation. The new operator Δ_{SP} plays an important role in the study of X-ray magnetic circular-dichroism (XMCD) spectra (Bouldi *et al.*, 2017; Kogo *et al.*, 2020).

A different approach based on the Gesztesy expansion can be applied to XAFS analyses. The one-electron Dirac Hamiltonian H_D for a potential V is written

$$H_{\mathrm{D}} = \begin{pmatrix} V + c^2 & c\sigma\cdot\mathbf{p} \\ c\sigma\cdot\mathbf{p} & V - c^2 \end{pmatrix}. \quad (57)$$

We can define a Green's function for the Dirac Hamiltonian,

$$G_{\rm D}(\varepsilon) = \frac{1}{\varepsilon + c^2 - H_{\rm D} + i\eta}. \quad (58)$$

As demonstrated by Gesztesy and coworkers, $G_{\rm D}(\varepsilon)$ is given by

$$\begin{aligned} G_{\rm D}(\varepsilon) &= \sum_{n=0}^{\infty} T^n \begin{bmatrix} g & gQ \\ Qg & QgQ + 1/(2c^2) \end{bmatrix}, \\ T &= \begin{pmatrix} 0 & X \\ 0 & Y \end{pmatrix}, \\ X &= gQ(V-\varepsilon), \\ Y &= [QgQ + 1/(2c^2)](V-\varepsilon), \\ Q &= \frac{\sigma\cdot\mathbf{p}}{2c}, \\ g(\varepsilon) &= \frac{1}{\varepsilon - T_{\rm e} - V + i\eta}. \end{aligned} \quad (59)$$

In equation (59), $g(\varepsilon)$ has no effects from the spin–orbit coupling, in contrast to $g(\varepsilon)$ in equation (54). The relativistic Green's function $G_{\rm D}$ is represented in terms of the non-relativistic Green's function g, which includes the potential V (Gesztesy *et al.*, 1984).

Substituting the Gesztesy expansion for the relativistic Green's function $G_{\rm D}$ in equation (51), we obtain a useful formula to describe the X-ray absorption intensity to include important relativistic effects,

$$\begin{aligned} I(\omega) &= I_1(\omega) + I_2(\omega), \\ I_1(\omega) &= -2{\rm Im}\Big[\langle\varphi_{\rm c}|\Delta_1^\dagger(g+\delta g)(\varepsilon)\Delta_1|\varphi_{\rm c}\rangle \\ &\quad + \langle\varphi_{\rm c}|\Delta_1^\dagger g(\varepsilon)Q\Delta_1|\chi_{\rm c}\rangle + \langle\chi_{\rm c}|\Delta_1^\dagger Qg(\varepsilon)\Delta_1|\varphi_{\rm c}\rangle\Big], \\ I_2(\omega) &= -2{\rm Im}\Big[\langle\varphi_{\rm c}|\Delta_1^\dagger g(\varepsilon)\Delta_2|\chi_{\rm c}\rangle + \langle\chi_{\rm c}|\Delta_2^\dagger g\Delta_1|\varphi_{\rm c}\rangle \\ &\quad + \langle\varphi_{\rm c}|\Delta_1^\dagger gQ\Delta_2|\varphi_{\rm c}\rangle + \langle\varphi_{\rm c}|\Delta_2^\dagger Qg\Delta_1|\varphi_{\rm c}\rangle\Big], \end{aligned} \quad (60)$$

$$\delta g(\varepsilon) = g(\varepsilon)Q(V-\varepsilon)Qg(\varepsilon). \quad (61)$$

In order to derive the Pauli equation from the Dirac equation, we use an approximation (Schwable, 2008),

$$|\chi_{\rm c}\rangle \approx Q|\varphi_{\rm c}\rangle. \quad (62)$$

Substituting equation (62) into equation (60), we obtain

$$\begin{aligned} I_1(\omega) &= -2{\rm Im}\Big[\langle\varphi_{\rm c}|\Delta_1^\dagger(g+\delta g)\Delta_1|\varphi_{\rm c}\rangle \\ &\quad + \langle\varphi_{\rm c}|\Delta_1^\dagger g\Delta_{\rm SP} + \Delta_{\rm SP}^\dagger g\Delta_1|\varphi_{\rm c}\rangle\Big], \\ I_2(\omega) &= -2{\rm Im}\Big[\langle\varphi_{\rm c}|\Delta_1^\dagger g\Delta_{\rm M1} + \Delta_{\rm M1}^\dagger g\Delta_1|\varphi_{\rm c}\rangle\Big]. \end{aligned} \quad (63)$$

We thus obtain quite a similar X-ray absorption formula as obtained in the framework of the FW transformation (see equation 54; Kogo *et al.*, 2020).

In the nonrelativistic limit ($c \to \infty$) only Δ_1 in I_1 (see equation 63) contributes to the X-ray absorption intensity. As pointed out by Brouder and coworkers, $Q(V-\varepsilon)Q$ in equation (61) is written

$$Q(V-\varepsilon)Q = -\frac{1}{4c^2}[\nabla V\cdot\nabla + (V-\varepsilon)\nabla^2] + \xi(r)\sigma\cdot\mathbf{L}, \quad (64)$$

where ξ for a spherically symmetric potential V is given by (Brouder *et al.*, 1996)

$$\xi(r) = \frac{1}{4c^2 r}\frac{{\rm d}V(r)}{{\rm d}r}.$$

The spin–orbit coupling term (the third term of equation 64) for photoelectrons can give a finite contribution to the K-edge XMCD. The first and the second terms in equation (64) can contribute to XANES spectra, but make no contribution to XMCD spectra.

So far, we have discussed one-electron relativistic XAFS theory. One of the important advantages of the Gesztesy expansion is its direct extension to many-body relativistic theory. A many-body relativistic theory for the analysis of XAFS spectra has been developed on the basis of the quantum electrodynamics (QED) Keldysh Green's function approach, in which photon Green's functions play an important role (Fujikawa, 2004, 2005).

In QED theory both electron and photon Green's functions are important to describe X-ray absorption processes.

The space components of the photon Green's function $D^{ij}(1,2)$ $(i,j = x,y,z)$ are given in terms of the vector potential fluctuations,

$$\begin{aligned} iD^{ij}(1,2) &= \frac{1}{4\pi}\langle T_{\rm c}[\delta A^i(1)\delta A^j(2)]\rangle, \\ \delta A^i(1) &= A^i(1) - \langle A^i(1)\rangle. \end{aligned} \quad (65)$$

The path-ordering operator $T_{\rm c}$ is used. We should note that the vector potentials A^i $(i = 1, 2, 3)$ are q-numbers. In QED, the absorption intensity $I(\omega)$ is given by use of the photon Green's function D,

$$\begin{aligned} I(\omega) &\propto -{\rm Im}\langle d^l(\lambda)|(P + PDP)^{>lm}(\omega)|d^m(\lambda)\rangle, \\ d^l(\lambda) &= \frac{1}{V^{1/2}}\exp(i\mathbf{k}\cdot\mathbf{r})e_l(\lambda), \end{aligned} \quad (66)$$

where $\mathbf{e}(\lambda)$ $(\lambda = \mathbf{k}, s)$ is the polarization vector of the X-rays (s stands for the polarization mode) and V is the volume of the normalization box. Here, the photon self-energy P is defined as the functional derivative of the average of the electron current density j^β with respect to the average of the vector potential operator A^α $(\alpha, \beta = 0, 1, 2, 3)$,

$$P_\alpha^\beta(1,2) = \frac{4\pi}{c}\frac{\delta\langle j^\beta(1)\rangle}{\delta\langle A^\alpha(2)\rangle}. \quad (67)$$

In the fundamental equation (66), only the spatial parts are used.

As long as we consider only the first term of P in equation (66), we obtain a similar XAFS formula to equation (63): g, however, has many-body effects in the electron retarded self-energy $\Sigma^{\rm r}$, which works as an optical potential for photoelectrons.

One of the outstanding features of the QED theory allows us to discuss radiation-field screening in XAFS spectra. We can show that

$$\langle d^l(\lambda)|(P+PDP)^{>lm}|d^m(\lambda)\rangle \propto \int \mathrm{d}\mathbf{r}_1\,\mathrm{d}\mathbf{r}_2\,\Delta^\dagger(\mathbf{r}_1)(P+PWP)^>(\mathbf{r}_1,\mathbf{r}_2;\omega)\Delta(\mathbf{r}_2), \quad (68)$$

where $P=P_0^0$ is the irreducible polarization used in non-relativistic many-body theory (Hedin & Lundqvist, 1970). Both P and W describe the electron–electron interaction. We now convert the time integration on the Keldysh path to the ordinary time integration from $-\infty$ to ∞; we have a useful formula to infinite order of the Coulomb interaction v,

$$(P+PWP)^> = (1-P^{\mathrm{r}}v)^{-1}P^>(1-vP^{\mathrm{a}})^{-1}, \quad (69)$$

where P^{a} is the advanced polarization. Substituting equation (69) into equation (66), we thus have an important relativistic XAFS formula,

$$I(\omega)\propto -\mathrm{Im}\langle\varphi_{\mathrm{c}}|\tilde{\Delta}^\dagger(\omega)G^{\mathrm{r}}(\varepsilon)\beta\tilde{\Delta}(\omega)|\varphi_{\mathrm{c}}\rangle, \quad (70)$$

where G^{r} is the relativistic 4×4 retarded Green's function and β is also a 4×4 diagonal matrix,

$$\beta=\begin{pmatrix}1 & 0\\ 0 & -1\end{pmatrix}.$$

We now define the dynamically screened electron–photon interaction $\tilde{\Delta}(\omega)$,

$$\tilde{\Delta}(\mathbf{r},\omega)=\int \mathrm{d}\mathbf{r}'\,(\varepsilon^{\mathrm{a}})^{-1}(\mathbf{r},\mathbf{r}';\omega)\Delta(\mathbf{r}'), \quad (71)$$

which explicitly depends on the photon energy ω. Radiation-field screening plays an important role in explaining the large deviation of the L_2 to L_3 branching ratio 1/2. Schwitalla and Ebert have developed an approach to study the above problem based on time-dependent DFT and the linear response formalism (Schwitalla & Ebert, 1998). Ankudinov and coworkers have also studied these problems taking account of the radiation-field screening within the linear approximation (Ankudinov *et al.*, 2003).

A full relativistic XANES theory using the KKR–Green's function method has been developed by Ebert *et al.* (2011).

6. Ultrafast XANES

Ultrafast XAFS measurements have been applied to study transient structures after laser pump excitation (Bressler & Chergui, 2004). These analyses are based on the assumption that ultrafast XAFS provides us with snapshot spectra. There is a question as to whether or not these analyses can be built on a sound theoretical basis. Ultrafast XAFS using X-ray free-electron lasers (XFELs) is very promising. Mukamel and coworkers have contributed to the development of pump–probe XAFS theory based on nonlinear response theory in Liouville space (Tanaka *et al.*, 2001; Mukamel, 2005; Healion *et al.*, 2008). A theory for the study of pump–probe ultrafast XAFS spectra has been proposed based on a nonrelativistic Keldysh Green's function approach which can incorporate both intrinsic and extrinsic losses and also resonant effects (Fujikawa & Niki, 2016).

Here, we study pump–probe XAFS. In the remote past it was assumed that the system is in the ground state $|0\rangle$. The full time evolution operator $U(t,t_0)$ is influenced by both the A and B operators, where A describes the interaction between the probe X-ray pulses from the XFEL and the electronic systems after the pump pulse irradiation. In addition to the probe X-rays, the pump laser is used to excite the target. The interaction between the pump pulse and the system is described by the operator B. The operators are explicitly given by

$$A(1)=a(t_1)\Delta(\mathbf{r}_1)+\mathrm{cc}, \quad (1=\mathbf{r}_1,t_1)$$
$$B(1)=b(t_1)\Delta(\mathbf{r}_1)+\mathrm{cc}. \quad (72)$$

The factors a and b show the time-dependence of the pulses: $a(t)$ is only nonzero in the interval $t_1<t<t_2$ and $b(t)\neq0$ in the interval $0<t<t_0$ ($t_0<t_1$). We now define the operator V_1 as

$$V_1(t_1)=\int \mathrm{d}\mathbf{r}_1\,\psi^\dagger(\mathbf{r}_1)A(1)\psi(\mathbf{r}_1) = a(t_1)\exp(-i\omega_\lambda t_1)\int \mathrm{d}\mathbf{r}_1\,\Delta(\mathbf{r}_1)n(\mathbf{r}_1). \quad (73)$$

We should note that A is much weaker than B. We thus fully keep B, whereas we keep only the lowest-order terms with respect to A, which yields the expansion of U,

$$U(t,t_0)=U_2(t,t_0)-i\int_{t_0}^{t}\mathrm{d}t_1\,U_2(t,t_1)V_1(t_1)U_2(t_1,t_0)+\cdots,$$
$$U_2(t,t_0)=T\exp\left\{-i\int_{t_0}^{t}\mathrm{d}t_1\left[H+\int \mathrm{d}\mathbf{r}_1\,\psi^\dagger(1)B(1)\psi(1)\right]\right\}. \quad (74)$$

The X-ray absorption probability of $\lambda=(\mathbf{k},s)$ photons at time t is now given by use of the second term of U in equation (74),

$$I_\lambda(t)=\sum_{n\neq0}\left|\langle n|\int_{t_0}^{t}\mathrm{d}t_1\,U_2(t,t_1)V_1(t_1)U_2(t_1,t_0)|0\rangle\right|^2 = \int_{t_0}^{t}\mathrm{d}t_1\int_{t_0}^{t}\mathrm{d}t_2\,a^*(t_1)a(t_2)\exp[i\omega_\lambda(t_1-t_2)] \times \int \mathrm{d}\mathbf{r}_1\,\mathrm{d}\mathbf{r}_2\,\Delta^*(\mathbf{r}_1)\Delta(\mathbf{r}_2)\langle0|\delta n(1)\delta n(2)|0\rangle, \quad (75)$$

which yields a basic formula to describe the pump–probe XAFS at time t,

$$I_\lambda(t)=\int_{t_0}^{t}\mathrm{d}t_1\int_{t_0}^{t}\mathrm{d}t_2\,a^*(t_1)a(t_2)\exp[i\omega_\lambda(t_1-t_2)] \times \int \mathrm{d}\mathbf{r}_1\,\mathrm{d}\mathbf{r}_2\,\Delta^*(\mathbf{r}_1)\Delta(\mathbf{r}_2)i\pi^>(1,2), \quad (76)$$

which is quite similar to equation (35). The pump pulse switches on at t_0. The reducible polarization π satisfies equation (36); however, it already includes the effects of pump pulse B, which is strong enough that we should go beyond weak perturbation theory.

The lowest-order approximation for $\pi^>$ is obtained by use of the skeleton expansion in terms of the dressed electron Green's function G_B (see also equation 37),

$$\pi(1,2)\approx P_0^>(1,2)=-ig_B^>(1,2)g_B^<(2,1). \quad (77)$$

The pump pulse is included in G_B, which satisfies the Dyson equation in Keldysh space,

$$\left[i\frac{\partial}{\partial t_1} - h(1) - B(1) - V_H(1)\right]G_B(1,2) - \int_c \mathrm{d}3\ \Sigma_B(1,3)G_B(3,2) = \delta_c(1,2), \quad (78)$$

where $\int_c$ represents integration over the closed time path, δ_c is the delta function on the closed path and Σ_B is the electron self-energy including the pump pulse B.

We now consider the no-loss channel for simplicity. The absorption intensity is given by use of the time-dependent intrinsic amplitude $S_0(t)$,

$$I_\lambda(t) = \mathrm{Re}\Big\{ \int_{t_0}^{t} \mathrm{d}t_1 \int_{t_0}^{t} \mathrm{d}t_2\, a^*(t_1)a(t_2)S_0(t_1)^* \times S_0(t_2)\exp[i\omega_\lambda(t_1 - t_2)] \int \mathrm{d}\mathbf{r}_1\, \mathrm{d}\mathbf{r}_2\, \varphi_c(\mathbf{r}_1)^* \times \Delta^*(\mathbf{r}_1)g_B^>(1,2)\Delta(\mathbf{r}_2)\varphi_c(\mathbf{r}_2)\Big\}. \quad (79)$$

The hole propagator $g_B^<$ can be given in terms of the time-dependent intrinsic amplitude $S_0(t)$, which includes the history of the system after pump excitation,

$$S_0(t) = \sum_j \langle 0^*|b|j\rangle\langle j|\hat{U}(t,t_0)|0\rangle \times \exp[i(E_0^* - E_0)(t - t_0)], \quad (80)$$

$$\hat{U}(t,t_0) = T\exp\Big[-i\int_{t_0}^{t}\mathrm{d}t_1\, B(1)\hat{n}(1)\Big],$$
$$\hat{n}(1) = \exp[iH(t_1 - t_0)]n(\mathbf{r}_1)\exp[-iH(t_1 - t_0)], \quad (81)$$

where $|0^*\rangle$ is the eigenstate of the hole Hamiltonian H_v^* and $|j\rangle$ and $|0\rangle$ are the eigenstates of the no-hole Hamiltonian H_v. The time-dependent Dyson orbitals are also used to study ultrafast photoemission spectra from molecules (Perveaux *et al.*, 2014; Spanner & Patchkovskii, 2009).

For practical purposes, the random-phase-approximation (RPA)–boson approach is introduced in order to derive time-dependent XAFS at a delay time t_A, which is given by (Fujikawa & Niki, 2016)

$$I_\lambda(t_A) \propto -|L_0(t_A)|^2 \times \mathrm{Im}\langle c|\Delta^* g_B^>[\varepsilon, Q(t_A)]\Delta|c\rangle, \quad (82)$$

$$|L_0(t_A)|^2 = 1 + 2\sum_p |C_p|\sin(\omega_p t_A - \theta_p), \quad (83)$$

where $|C_p|$ and θ_p are energy-dependent parameters for the pth boson with energy $\omega_p > 0$. The instantaneous atomic configuration at time t_A is denoted $Q(t_A) = [\mathbf{R}_1(t_A), \mathbf{R}_2(t_A), \ldots]$. The factor $-\mathrm{Im}\langle c|\Delta^* g_B^>\Delta|c\rangle$ reflects the averaged structure $Q(t_A)$ around an X-ray-absorbing atom, which can differ from that in the ground electronic state. The new factor $|L_0(t_A)|^2$ shows rapid oscillation as a function of the delay t_A; ω_p is of the order of a few eV. These rapid oscillations caused by the pump pulse excitation can provide us with useful information on excited electronic structures and dynamics of the systems. These rapid oscillations, however, should be redundant in obtaining the time-dependent structural change after the pump pulse irradiation.

7. Bethe–Salpeter equation

The formula (35) accurately describes the XAS processes. The reducible polarization π satisfies equation (36). The polarization π is related to the density correlation function L, which is a solution of the integral equation called the Bethe–Salpeter equation in Keldysh space (Bechstedt, 2015; Strinati, 1988),

$$L(12;1'2') = G(1,2')G(2,1') + \int_c \mathrm{d}3\ldots\mathrm{d}6\, G(1,3)G(4,1')\Xi(36,45)L(52,62'), \quad (84)$$

where

$$\Xi(36,45) = -i\delta_c(3,4)v_c(3,5)\delta_c(5,6) + \frac{\delta\Sigma(3,4)}{\delta G(5,6)}. \quad (85)$$

In some special cases L is related to other functions such as the polarization π,

$$L(12,1^+2^+) = i\pi(1,2). \quad (86)$$

The Bethe–Salpeter (BS) equation (84) for L is much more complicated compared with the Dyson equation (36) for π. Combining equations (84) and (86) gives the same results for the XAS analyses as the reducible polarization π in equation (35). In the low-order approximation, however, they can give different results.

Ankudinov and coworkers presented a combined approach of the BS equation and the time-dependent DFT theory for XANES calculations (Ankudinov *et al.*, 2005). They found that their combined approach worked well both for cases in which the local field effect dominates, for example tungsten, and in which the core-hole interaction dominates, for example MgO. Rehr and coworkers compared the BS equation approach with the final-state rule to handle core-hole effects within the independent electron approximation (Rehr *et al.*, 2005).

The BS equations have been applied to optical properties of solids (Strinati, 1988) with remarkable success, but they require quite a large-scale computation. On the other hand, equation (35) partly includes radiation-field screening (see equations 70 and 71). If we go beyond the lowest order of the irreducible polarization P, we can include the electron–hole interaction.

8. Conclusion

A brief review of XANES theories has been given which focuses on the basic theoretical framework rather than the technical details. Depending on the different theoretical approaches, some different physical aspects are stressed.

Because of the limited space for this chapter, we cannot discuss the XANES measured using X-ray Raman scattering (Schülke, 2007) and electron energy losses (EELS; Fujikawa, 2002).

References

Almbladh, C. O. & Hedin, L. (1983). *Handbook on Synchrotron Radiation*, edited by E. E. Koch, Vol. 1b, pp. 607–904. Amsterdam: North-Holland.

Ankudinov, A. L., Nesvizhskii, A. I. & Rehr, J. J. (2003). *Phys. Rev. B*, **67**, 115120.

Ankudinov, A. L. & Rehr, J. J. (1997). *Phys. Rev. B*, **56**, R1712–R1716.

Ankudinov, A. L. & Rehr, J. J. (2005). *Phys. Scr.* **2005**, 24.

Ankudinov, A. L., Takimoto, Y. & Rehr, J. J. (2005). *Phys. Rev. B*, **71**, 165110.

Bechstedt, F. (2015). *Many-Body Approach to Electronic Excitations*. Berlin, Heidelberg: Springer-Verlag.

Bouldi, N. & Brouder, C. (2017). *Eur. Phys. J. B*, **90**, 246.

Bouldi, N., Vollmers, N. J., Delpy-Laplanche, C. G., Joly, Y., Juhin, A., Sainctavit, P., Brouder, C., Calandra, M., Paulatto, L., Mauri, F. & Gerstmann, U. (2017). *Phys. Rev. B*, **96**, 085123.

Bressler, C. & Chergui, M. (2004). *Chem. Rev.* **104**, 1781–1812.

Brouder, C., Alouani, M. & Bennemann, K. H. (1996). *Phys. Rev. B*, **54**, 7334–7349.

Brouder, C., Cabaret, D., Juhin, A. & Sainctavit, P. (2010). *Phys. Rev. B*, **81**, 115125.

Brouder, C. & Hikam, M. (1991). *Phys. Rev. B*, **43**, 3809–3820.

Cabaret, D. & Brouder, C. (2009). *J. Phys. Conf. Ser.* **190**, 012003.

Campbell, L., Hedin, L., Rehr, J. J. & Bardyszewski, W. (2002). *Phys. Rev. B*, **65**, 064107.

Ebert, H. (1996). *Rep. Prog. Phys.* **59**, 1665–1735.

Ebert, H., Ködderitzsch, D. & Minár, J. (2011). *Rep. Prog. Phys.* **74**, 096501.

Ebert, H., Popescu, V. & Ahlers, D. (1999). *Phys. Rev. B*, **60**, 7156–7165.

Fornasini, P. (2012). *e-J. Surf. Sci. Nanotechnol.* **10**, 480–485.

Fritzsche, V. (1990). *J. Phys. Condens. Matter*, **2**, 9735–9747.

Fujikawa, T. (1993). *J. Phys. Soc. Jpn*, **62**, 2155–2165.

Fujikawa, T. (1999). *J. Phys. Soc. Jpn*, **68**, 2444–2456.

Fujikawa, T. (2001). *J. Synchrotron Rad.* **8**, 76–80.

Fujikawa, T. (2002). *Handbook on Thin Film Materials*, edited by H. S. Nalwa, Vol. 2, pp. 415–477. New York: Academic Press.

Fujikawa, T. (2004). *J. Electron Spectrosc. Relat. Phenom.* **136**, 85–98.

Fujikawa, T. (2005). *Phys. Scr.* **2005**, 35.

Fujikawa, T., Hatada, K. & Hedin, L. (2000). *Phys. Rev. B*, **62**, 5387–5398.

Fujikawa, T. & Hedin, L. (1989). *Phys. Rev. B*, **40**, 11507–11518.

Fujikawa, T. & Niki, K. (2016). *J. Electron Spectrosc. Relat. Phenom.* **206**, 74–85.

Fujikawa, T., Sakuma, H., Niki, K. & Sébilleau, D. (2015). *J. Electron Spectrosc. Relat. Phenom.* **198**, 57–67.

Gesztesy, F., Grosse, H. & Thaller, B. (1984). *Ann. Inst. Henri Poincaré*, **40**, 159–174.

Hara, S. (1967). *J. Phys. Soc. Jpn*, **22**, 710–718.

Hatada, K. & Natoli, C. R. (2018). *Multiple Scattering Theory for Spectroscopies*, edited by D. Sébilleau, K. Hatada & H. Ebert, pp. 67–91. Cham: Springer Nature Switzerland.

Healion, D. M., Schweigert, I. V. & Mukamel, S. (2008). *J. Phys. Chem. A*, **112**, 11449–11461.

Hedin, L. (1988). *Recent Progress in Many-Body Theories*, Vol. 1, edited by A. J. Kallio, E. Pajanne & R. F. Bishop, pp. 307–316. New York, London: Plenum Press.

Hedin, L. (1989). *Physica B*, **158**, 344–346.

Hedin, L. & Lundqvist, B. I. (1971). *J. Phys. C Solid State Phys.* **4**, 2064–2083.

Hedin, L. & Lundqvist, S. (1970). *Solid State Phys.* **23**, 1–181.

Kogo, J., Niki, K. & Fujikawa, T. (2020). *J. Phys. Soc. Jpn*, **89**, 064709.

Kosugi, N., Yokoyama, T., Asakura, K. & Kuroda, H. (1984). *Chem. Phys.* **91**, 249–256.

Krüger, P. (2018). *Multiple Scattering Theory for Spectroscopies*, edited by D. Sébilleau, K. Hatada & H. Ebert, pp. 143–169. Cham: Springer Nature Switzerland.

Laan, G. van der (2006). *Magnetism: A Synchrotron Radiation Approach*, edited by E. Beaurepaire, H. Bulou, F. Scheurer & J.-P. Kappler, pp. 143–199. Berlin, Heidelberg: Springer-Verlag.

Lee, P. A. & Beni, G. (1977). *Phys. Rev. B*, **15**, 2862–2883.

Manuel, D., Cabaret, D., Brouder, C., Sainctavit, P., Bordage, A. & Trcera, N. (2012). *Phys. Rev. B*, **85**, 224108.

Minar, J., Sipr, O., Braun, J. & Ebert, H. (2018). *Multiple Scattering Theory for Spectroscopies*, edited by D. Sébilleau, K. Hatada & H. Ebert, pp. 93–142. Cham: Springer Nature Switzerland.

Mukamel, S. (2005). *Phys. Rev. B*, **72**, 235110.

Natoli, R., Benfatto, M., Brouder, C., López, M. F. R. & Foulis, D. L. (1990). *Phys. Rev. B*, **42**, 1944–1968.

Nemausat, R., Cabaret, D., Gervais, C., Brouder, C., Trcera, N., Bordage, A., Errea, I. & Mauri, F. (2015). *Phys. Rev. B*, **92**, 144310.

Nozawa, S., Iwazumi, T. & Osawa, H. (2005). *Phys. Rev. B*, **72**, 121101.

Perveaux, A., Lauvergnat, D., Lasorne, B., Gatti, F., Robb, M. A., Halász, G. J. & Vibók, A. (2014). *J. Phys. B At. Mol. Opt. Phys.* **47**, 124010.

Rehr, J. J. & Albers, C. R. (1990). *Phys. Rev. B*, **41**, 8139–8149.

Rehr, J. J. & Albers, C. R. (2000). *Rev. Mod. Phys.* **72**, 621–654.

Rehr, J. J., Soininen, J. A. & Shirley, E. L. (2005). *Phys. Scr.* **2005**, 207.

Schülke, W. (2007). *Electron Dynamics by Inelastic X-ray Scattering*. Oxford University Press.

Schwable, F. (2008). *Advanced Quantum Mechanics*, 4th ed., pp. 181–194. Berlin, Heidelberg: Springer-Verlag.

Schwitalla, J. & Ebert, H. (1998). *Phys. Rev. Lett.* **80**, 4586–4589.

Shinotsuka, H., Arai, H. & Fujikawa, T. (2008). *Phys. Rev. B*, **77**, 085404.

Slater, J. C. (1951). *Phys. Rev.* **81**, 385–390.

Spanner, M. & Patchkovskii, S. (2009). *Phys. Rev. A*, **80**, 063411.

Strinati, G. (1988). *Riv. Nuovo Cim.* **11**, 1–86.

Tanaka, S., Chernyak, V. & Mukamel, S. (2001). *Phys. Rev. A*, **63**, 063405.

Wende, H. (2004). *Rep. Prog. Phys.* **67**, 2105–2181.